Petroleum Science
https://doi.org/10.1007/s12182-020-00487-1

ORIGINAL PAPER

Hydrocarbon generation from lacustrine shales with retained oil during thermal maturation

Xin-He Shao[1,2] · Xiong-Qi Pang[1,2] · Mao-Wen Li[3,4] · Zhi-Ming Li[4] · Yi Zhao[1,2]

Received: 7 January 2020

Abstract

Thermal maturation in the shale oil/gas system is inherently complex due to the competitive interplays between hydrocarbon generation and retention processes. To study hydrocarbon generation characteristics from shales within different stages of thermal maturation under the influence of retained oil, we performed Micro-Scale Sealed Vessels (MSSV) pyrolysis on a set of artificially matured lacustrine shale samples from the Shahejie Formation in the Dongpu Depression in Bohai Bay Basin, China. Experimental results show that hydrocarbon yields of shale samples with or without retained oil at various thermal maturities follow different evolution paths. Heavy components (C_{15+}) in samples crack at high temperatures and generally follow a sequence, where they first transform into C_{6-14} then to C_{2-5} and C_1. Methane accounts for most of the gaseous products at high temperatures in all samples, with different origins. The cracking of C_{2-5} is the main methane-generating process in samples with retained oil, whereas the source of methane in samples without retained oil is kerogen. In the studied shales, retained oils at early-mature stage retard the transformation of liquid to gaseous hydrocarbon and prompt the cracking of C_{2-5} to C_1 to some extent. TSR reaction related to gypsum in the studied samples is the primary reason that can explain the loss of hydrocarbon yields, especially at high temperatures. In addition, transformation of volatile hydrocarbons to gas and coke also accounts for the loss of generated hydrocarbon, as a secondary factor.

Keywords MSSV pyrolysis · Hydrocarbon generation · Lacustrine shales · Thermal maturation · Retained oil

1 Introduction

Hydrocarbon generation has been a topic of long-standing interest of petroleum geologists, and researchers have earned a lot of achievements in the last few decades (Tissot and Welte 1978; Lewan and Roy 2011; Sondergeld et al. 2013). The general scheme proposed by Tissot and Welte (1978) describing hydrocarbon formation during burial of source rocks has been widely accepted, and numerous studies were carried out on this basis. In addition, techniques have been improved greatly these years to analyze hydrocarbon generation from source rocks. Rock–Eval pyrolysis, gold tube pyrolysis, Micro-Scale Sealed Vessels (MSSV) pyrolysis, semi-closed and closed-system hydrous pyrolysis are more and more common in laboratories (Lewan and Roy 2011; Behar et al. 1992; Horsfield et al. 1989; Peters et al. 2006; Wu et al. 2016). By heating organic matter at high temperatures for short times, these techniques can successfully simulate hydrocarbon generation processes that occur at lower temperature and rather long time in geological conditions (Spigolon et al. 2015). Thanks to the efforts that researchers have taken, we have a generally clear understanding on the properties of kerogens and hydrocarbon products at all stages of thermal maturation. Also, differences of hydrocarbon generation characteristics among kerogens from

Edited by Jie Hao

✉ Xiong-Qi Pang
pangxq@cup.edu.cn

[1] State Key Laboratory of Petroleum Resources and Prospecting, China University of Petroleum, Beijing 102249, China

[2] College of Geosciences, China University of Petroleum, Beijing 102249, China

[3] State Key Laboratory of Shale Oil and Shale Gas Resources and Effective Development, SINOPEC Petroleum Exploration and Production Research Institute, Beijing 100083, China

[4] SINOPEC Key Laboratory of Petroleum Accumulation Mechanisms, Wuxi Institute of Petroleum Geology, Wuxi 214126, Jiangsu, China

Published online: 04 September 2020

various sedimentary settings have been recognized (Braun et al. 1991; Burnham 1989).

Nowadays, as shale oil and gas, which are hydrocarbons retained in source rocks, are gaining increasingly important positions in fuel energy. The relationship between hydrocarbon generation, retention and expulsion has become an issue receiving much attention (Jia et al. 2014; Han et al. 2015; Ziegs et al. 2017). None of these three processes can be considered as independent, because they interact with each other during thermal maturation. Some studies report that hydrocarbon expulsion efficiency plays an important role on resource abundance in a shale oil/gas layer (Jarvie et al. 2007; Jia et al. 2014; Li et al. 2015). Petroleum geologists have found that retained oil in shales influences not only the gas generation potential at high maturities, but also the chemical compositions of gaseous products (Gai et al. 2015; Pan et al. 2012). In addition, researchers have stated that oil and gas released during hydrocarbon generation may attach to kerogens (Erdmann and Horsfield 2006; Mahlstedt et al. 2008; Vu et al. 2008). This recombination between hydrocarbon and kerogen structures at low thermal maturity can affect hydrocarbon generation at high maturity in different ways, depending on the types and thermal maturities of organic matters. Gai et al. (2015) used mixtures of immature kerogens and artificially matured oils in their pyrolysis experiments. The results suggested that interactions between kerogens and residual oils during hydrocarbon generation do not change total gas generation potential. Pan et al. (2012) conducted closed-system pyrolysis in gold tubes using mixed oil and pyrobitumen and suggested that existence of pyrobitumen can prompt methane generation by oil cracking. Compared to siliciclastic sandstones and carbonate rocks, shales have more diverse chemically unstable minerals, such as clay minerals, gypsum, halite. These inorganic minerals may also play a part in hydrocarbon generation by reacting with fluids or kerogens in shales. It is documented in some laboratory works that rock fabric can catalyze hydrocarbon generation (Rahman et al. 2018; Shao et al. 2018a, b). Overall, hydrocarbon generation in a shale play can be quite a complicated story. More works are needed on issues related to how exactly do organic and inorganic components in shales act during thermal maturation.

On the basis of previous studies, we tried to work out how retained oils with different thermal maturities affect the late hydrocarbon generation. By conducting MSSV pyrolysis experiments on shale samples with or without retained oil, the purpose of this research is attained from three aspects: (1) investigating hydrocarbon generation characteristics of a lacustrine shale throughout the thermal maturation process; (2) finding out the compositional differences between hydrocarbons generated from extracted and unextracted samples; and (3) studying how hydrocarbon yields from samples within different thermal maturity evolve when heating to different temperatures. In addition, to answer whether inorganic minerals affect hydrocarbon generation of lacustrine shales, we also use a kerogen sample for comparative study. Results from this study are expected to provide theoretical guidance in oil resource assessment of lacustrine shales.

2 Samples and experiments

2.1 Sample preparation

An immature shale core sample from the third member of Eocene Shahejie Formation (Es_3) in the Dongpu Depression in the Bohai Bay Basin, China, is used for sample preparation in this study. This sample has a burial depth of 1777 m. The Es_3 is considered as a major shale oil–gas exploration target in the Dongpu Depression. It is dominated by laminated organic-rich shales and gypsum-salt beds deposited in semi-deep and deep lacustrine settings (Shao et al. 2018a, b). The sample consists mainly of clay minerals (42.0 wt%) and quartz (25.1 wt%), as well as gypsum (15.0 wt%), carbonate minerals (calcite: 4.7 wt%; dolomite: 5.7 wt%), pyrite (6.5 wt%) and halite (1.1 wt%). The sample has a total organic carbon (TOC) content of 2.13 wt%, a measured vitrinite reflectance (R_o) of 0.46% (Table 1), and contains dominantly type I kerogens with minor type III kerogens. Geological settings and detailed sample information are documented in Shao et al. (2018a, b, 2020). In addition, bitumen is found in this sample, which could be mixture of migrated-in oil and early generated bitumen according to the saturates, aromatics, resins and asphaltenes (SARA) compositions (Table 1).

Fifty grams of the sample was treated with HCl and HF to obtain kerogen. Remnant shale sample was separated into three aliquots and crushed into fragments. Two aliquots of the shale fragments were heated in a semi-open hydrous pyrolysis system at 325 °C and 350 °C isothermally for 48 h, respectively. By simulating hydrocarbon generation and expulsion from organic matters, semi-open hydrous pyrolysis can reflect complex thermal maturation process under geological conditions. To set boundary conditions in the semi-open hydrous pyrolysis, we referred to burial and thermal history of the area where the studied sample is from. Data were provided by Sinopec Zhongyuan Oilfield Company. In this way, oil-bearing samples with different thermal maturities, which can generally reflect hydrocarbon generation and expulsion in geological conditions, were obtained (Shao et al. 2020). Next, heated samples were crushed into powders (about 100 mesh), and each aliquot of samples was further divided into two aliquots, with one aliquot subjected to solvent extraction (dichloromethane, 72 h) to remove the retained oil in samples. SARA compositions in extracts were separated using column chromatography. Heated extracted samples were also treated with HCl and HF to

Table 1 Organic geochemical parameters of samples used in the MSSV pyrolysis experiment

	Sample0-un	Sample0-ex	Sample325-un	Sample325-ex	Sample350-un	Sample350-ex	Sample-k
TOC, wt%	2.13	1.95	2.52	1.44	2.24	1.35	19.66
S2, mg/g	7.39	7.17	8.13	1.07	4.96	0.59	67.55
S1, mg/g	0.88	–	1.95	–	1.76	–	
Retained oil*, mg/g	1.10	–	9.01	–	6.13	–	–
Saturate, %	41.74	–	34.80	–	45.19	–	–
Aromatic, %	9.61	–	14.42	–	13.78	–	–
Resin, %	39.04	–	27.27	–	25.64	–	–
Asphaltene, %	9.61	–	23.51	–	15.38	–	–
R_o, %	–	0.46	–	1.37	–	1.62	–

– no data

*Retained oil $= S1_{unextracted} + S2_{unextracted} - S2_{extracted}$ (Han et al. 2015)

obtain kerogen for R_o measurement. R_o values of sample and SARA compositions of retained oils can be found in Table 1.

2.2 MSSV pyrolysis and products analysis

MSSV pyrolysis was performed on the above-mentioned samples (two unheated whole-rock samples, four heated whole-rock samples and one kerogen sample). Apparatus and procedure of the MSSV pyrolysis are described in detail in the work of Horsfield and Dueppenbecker (1991). Here, 4–5 mg whole-rock samples or < 1 mg kerogen samples were loaded into glass tubes. Clean silicon sands were added in tubes to fill in void volumes. The glass tubes were sealed with H_2 flame and heated in a MSSV Sample Preparation Oven from room temperatures (23 °C) at a rate of 2 °C/min. The target heating temperatures for Sample-k, Sample0-un, Sample0-ex, Sample 325-un and Sample325-ex are 350, 375,400, 425, 450, 475, 500, 525, 550, 575, 600 °C, while for Sample 350-un and Sample350-ex are 375, 400, 425, 450, 475, 500, 525, 550, 575, 600 °C. Glass tubes were removed from the oven once they reached target temperatures and cooled down.

Generated hydrocarbon products from MSSV pyrolysis were quantitatively analyzed using an Agilent GC 7890B gas chromatograph (GC) apparatus equipped with a flame ionization detector (FID). Glass tubes were cracked open by a piston device in helium atmosphere at 300 °C, and pyrolysis products are able to transferred into a liquid N_2 cold trap for collection. These products were then released by heating the GC oven. The GC oven temperature was programmed to held at 40 °C for 13 min and then increases toward 320 °C with a heating rate of 5 °C/min, and isotherm time is 25 min for final temperature. At the first 9 min of the program, liquid N_2 was used to keep trap temperature lower than boiling points of most hydrocarbons, while only methane could come out from the trap. Liquid N_2 was removed afterward for the release of other hydrocarbon products. Hydrocarbon components are identified and quantified with GC ChemStation© software from Agilent Technologies.

3 Results

Yields of generated hydrocarbons during MSSV pyrolysis are summarized in Table 2, and details are described in the following sections.

3.1 Pyrolysis products from the unheated samples

The cumulative yields of total hydrocarbon products and different fractions including C_1, C_{2-5}, C_{6-14} and C_{15+} from Sample0-ex and Sample0-un are shown in Fig. 1. Total hydrocarbon yields of both samples reach their maximum at about 550 °C (temperature of maximal yields cannot be told exactly because there are 25 °C gaps between individual heating temperatures). The total yield from Sample0-un increases progressively to 177.85 mg/g TOC with temperature increasing toward 550 °C. In comparison, the total yield from Sample0-ex displays a sharp increase from 33.09 mg/g TOC to 136.84 mg/g TOC in temperature range of 500 °C–550 °C. C_1 yield of Sample0-un reaches a maximum at 575 °C and then decreases slightly, while that of Sample0-ex maximizes at 550 °C and drops sharply at higher temperature. For Sample0-un, maximal yield of C_{6-14} appears at lower temperature than C_{2-5} components, while the evolution trends of C_{2-5} and C_{6-14} from Sample0-ex are similar. C_{15+} products of Sample0-un reach the maximal value at 425–450 °C, while the evolution of C_{15+} yields from Sample0-ex shows a flat curve throughout the heating series.

Histograms showing percentages of hydrocarbon products from Sample0-un and Sample0-ex have generally similar appearance with C_1 and C_{15+}. C_1 increases and C_{15+} decreases with increasing temperature, which indicates that the hydrocarbon products tend to transform from high

Table 2 Hydrocarbon yields of the unheated and artificially matured shale samples in the MSSV pyrolysis experiment

Temperature, °C	Yield, mg/g TOC										Calculated yield from per unit retained oil, mg/g Oil*			
	Total	C_1	C_{2-5}	C_{6-14}	C_{15+}	Total	C_1	C_{2-5}	C_{6-14}	C_{15+}	C_1	C_{2-5}	C_{6-14}	C_{15+}
	Sample0-un					Sample0-ex								
350	8.42	0.07	1.05	0.25	7.05	4.92	0.97	0.33	0.43	3.18				
375	7.38	1.24	0.52	0.76	4.85	10.15	2.09	0.64	1.54	5.90				
400	17.78	2.63	0.50	1.58	13.06	7.11	0.61	0.52	1.54	4.44				
425	45.66	8.24	1.37	10.26	25.79	18.13	4.54	1.14	6.55	5.90				
450	63.65	18.27	4.69	17.06	23.63	20.94	8.59	0.83	7.32	4.21				
475	84.71	31.05	10.58	31.01	12.05	27.16	11.37	3.76	10.60	1.43				
500	142.20	86.40	15.26	35.09	5.44	33.09	23.80	0.97	7.96	0.35				
525	166.20	99.58	26.44	33.83	6.35	97.26	59.64	12.61	21.59	3.42				
550	177.85	117.00	23.18	27.70	9.96	136.84	88.56	17.03	28.97	2.27				
575	170.73	132.02	12.43	21.50	4.78	84.78	61.37	6.23	15.83	1.35				
600	149.64	126.07	11.43	4.57	7.57	67.52	49.21	10.27	2.95	5.08				
	Sample325-un					Sample325-ex								
350	24.56	1.21	0.30	1.68	21.37	1.08	0.16	0.47	0.15	0.29	3.11	0.08	4.46	59.32
375	23.11	0.59	0.16	1.00	21.35	1.98	0.82	0.27	0.52	0.37	0.36	0.03	1.95	59.13
400	24.18	1.42	0.47	2.08	20.22	3.79	1.67	0.73	1.39	0.00	1.29	0.16	3.59	56.55
425	31.52	4.83	1.00	5.32	20.38	3.50	1.79	0.46	0.99	0.27	10.65	2.06	13.29	56.56
450	51.77	12.60	7.23	14.19	17.75	4.75	2.84	0.69	1.21	0.00	30.70	19.10	37.76	49.63
475	83.98	44.46	4.62	28.04	6.86	9.35	6.78	0.95	1.62	0.00	113.50	11.41	75.82	19.20
500	100.85	56.80	15.83	24.19	4.04	12.26	9.20	1.48	1.57	0.00	144.15	41.91	65.13	11.29
525	104.48	75.74	6.52	20.60	1.63	21.04	16.94	1.93	2.17	0.00	184.75	15.15	54.14	4.55
550	109.77	79.91	9.28	19.38	1.20	24.87	20.14	2.71	2.02	0.00	191.31	21.62	50.99	3.37
575	76.65	62.62	3.14	10.09	0.80	12.17	10.71	1.08	0.38	0.00	158.02	7.06	27.61	2.25
600	58.50	48.56	3.85	5.72	0.37	12.81	11.07	1.42	0.32	0.00	118.13	8.49	15.48	1.05
	Sample350-un					Sample350-ex								
375	24.13	0.39	0.24	0.55	22.96	6.13	0.73	0.51	0.42	4.48	−0.19	−0.26	1.08	74.05
400	21.62	1.64	0.27	1.76	17.95	5.15	1.24	0.61	0.89	2.41	3.27	−0.36	4.47	60.27
425	25.50	2.52	0.42	4.28	18.28	6.58	2.56	1.36	1.69	0.97	3.56	−1.44	11.90	64.67
450	27.32	7.47	2.49	8.58	8.78	6.79	4.08	1.31	1.40	0.00	18.32	6.22	28.27	32.07
475	32.70	17.00	2.99	11.01	1.70	13.59	9.14	1.87	2.58	0.00	41.98	6.79	34.57	6.23
500	59.49	41.42	4.08	12.36	1.63	14.16	11.19	1.57	1.41	0.00	126.72	11.45	42.07	5.96
525	63.07	47.13	5.11	10.46	0.37	19.08	14.73	1.61	1.72	1.01	139.79	15.13	34.42	−0.86
550	66.27	51.92	4.69	9.17	0.49	33.46	27.11	3.59	2.56	0.21	130.01	9.25	27.88	1.32
575	59.49	48.55	3.85	7.08	0.00	30.45	26.69	2.24	1.52	0.00	118.65	9.14	22.52	0.00
600	45.54	39.66	3.12	2.76	0.00	21.31	19.55	1.43	0.34	0.00	101.88	8.27	9.34	0.00
	Sample-k													
350	17.92	1.73	0.17	0.68	15.35									
375	34.94	3.65	0.33	2.12	28.83									
400	57.05	6.84	1.72	6.73	41.76									
425	76.23	13.22	5.27	16.67	41.07									
450	105.96	29.69	5.15	24.63	46.49									
475	112.08	36.64	19.27	38.68	17.49									
500	138.70	49.28	42.23	39.26	7.92									
525	173.63	84.71	36.08	40.99	11.85									
550	170.53	99.69	22.18	38.02	10.64									
575	168.45	107.43	19.09	33.18	8.75									
600	156.58	110.03	10.14	26.30	10.11									

Negative values marked with underlines may result from heterogeneity of the studied samples and small loading amounts of samples in each set of heating

*Calculated yield from per unit retained oil = $1000 \times (\text{Yield}_{un} \times \text{TOC}_{un} - \text{Yield}_{ex} \times \text{TOC}_{ex})$/Retained oil

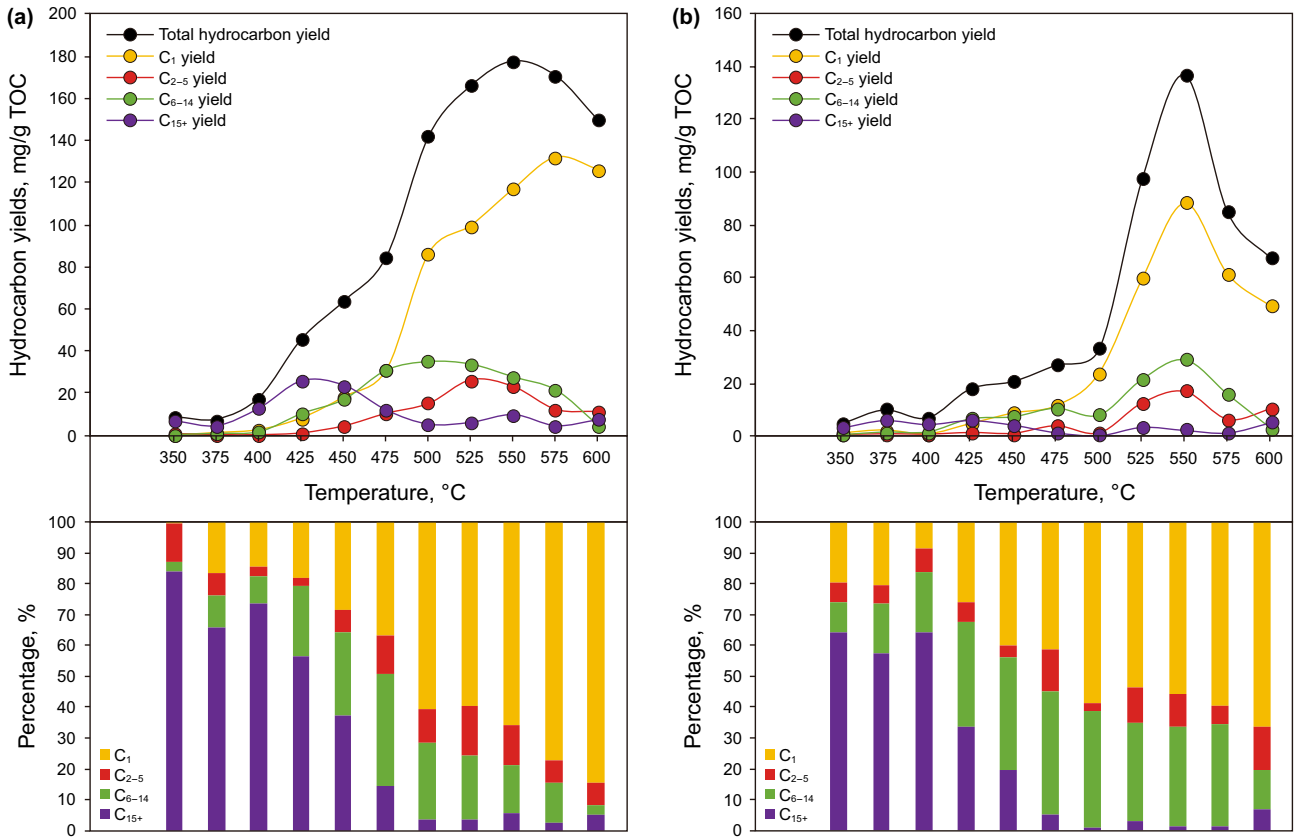

Fig. 1 Cumulative yields and percentages of C_1, $C_{2–5}$, $C_{6–14}$ and C_{15+} from MSSV Pyrolysis of Sample0-un (**a**) and Sample0-ex (**b**)

molecular weight into low molecular weight components during thermal maturation. A difference in aspect of the evolution of $C_{6–14}$ is worth noticing. At high-temperature range (> 500 °C), the percentage of $C_{6–14}$ products from Sample0-ex remains stable until about 575 °C, compared to those from Sample0-un which decrease gradually.

3.2 Pyrolysis products from the samples heated to 325 °C

Sample325-un is the one that has the highest retained oil content (9.01 mg/g) among the studied samples, and the R_o datum indicates that this sample is at the transition from oil to gas window. Maximal total and C_1 yields of Sample325-un and Sample325-ex all occur at around 550 °C (Fig. 2). For Sample325-un, yields of $C_{6–14}$ maximize at about 475 °C and $C_{2–5}$ yields reach the maximum at about 500 °C. Differently, the highest contents of $C_{2–5}$ and $C_{6–14}$ components from Sample325-ex both appear at about 550 °C, which are higher than those of Sample325-un. C_{15+} components of Sample325-ex remain at low contents during the entire heating series (< 0.5 mg/g TOC), indicating a limited generation potential of large molecular weight hydrocarbons. In contrast, C_{15+} components take up most of hydrocarbon yields from Sample325-un at heating temperatures lower than 425 °C, which is from the retained oil in samples. Here, an abrupt decrease of C_{15+} yield from 450 °C to 475 °C is notable, companied by increasing of low molecular hydrocarbons such as C_{6-14} and C_1.

Histograms of percentages of different hydrocarbon fractions from Sample325-un and Sample325-ex differ significantly from each other (Fig. 2). Light hydrocarbons ($C_{1–5}$) take predominance in total yields of Sample325-un after the heating temperature is larger than 475 °C, while they are dominant products in the entire heating series for Sample325-ex. The percentage of $C_{6–14}$ from Sample325-un increases as heating temperature increases to 475 °C, and then decreases slightly or remain stable. In Sample325-ex, the percentage of $C_{6–14}$ reaches a maximum at as early as 400 °C and then decreases gradually with increasing temperature. C_{15+} is the most important product of yield from Sample325-un at low temperatures and disappears at high heating temperatures. For Sample325-ex, the percentages of C_{15+} are low all the way.

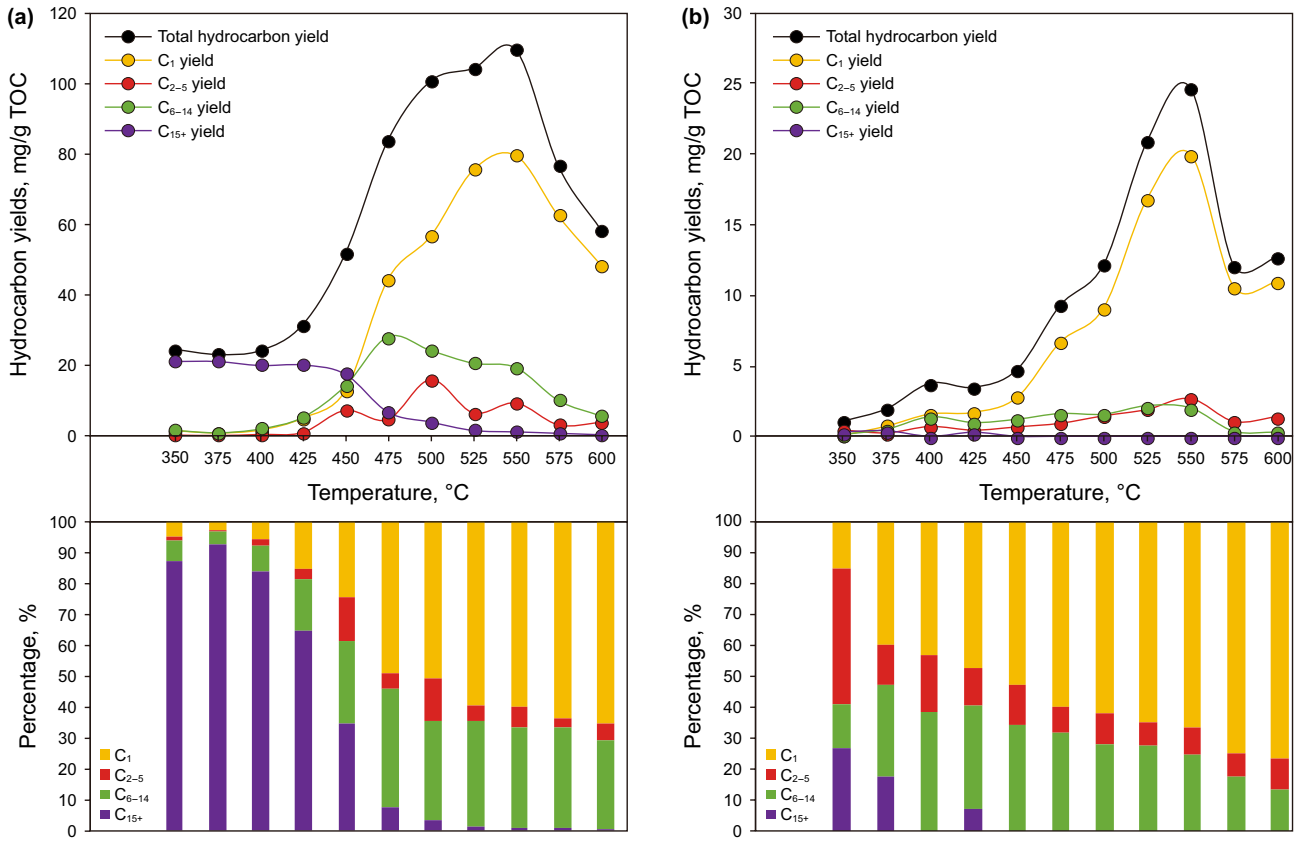

Fig. 2 Cumulative yields and percentages of C_1, $C_{2–5}$, $C_{6–14}$ and C_{15+} from MSSV pyrolysis of Sample325-un (**a**) and Sample325-ex (**b**)

3.3 Pyrolysis products from the samples heated to 350 °C

Samples heated to 350 °C have the highest thermal maturity ($R_o = 1.62\%$) among the samples in this study and contain residual hydrocarbon with a content of 6.13 mg/g. Similar to Sample325-un and Sample325-ex, the maximal values of total and C_1 yields from Sample350-un and Sample350-ex appear at around 550 °C (Fig. 3). $C_{2–5}$ components of Sample350-un increase with increasing temperature toward 525 °C and then remain stable until 600 °C. $C_{6–14}$ fractions from Sample350-un increase with increasing heating temperature till 500 °C and decrease gradually afterward. For Sample350-ex, $C_{2–5}$, $C_{6–14}$ and C_{15+} yield keep remaining in low contents (< 5 mg/g TOC). C_{15+} yields from Sample350-un are high at low heating temperature and decrease quickly from 4.48 mg/g TOC to 0 mg/g TOC during the heating range of 375 °C–475 °C, accompanied with increases of C_1, $C_{2–5}$, $C_{6–14}$ yields.

According to the histograms showing percentages of yields of different fractions from Sample350-un and Sample350-ex, some differences can be found (Fig. 3). Percentages of $C_{2–5}$ yields from Sample350-ex reach a maximum at about 425 °C, while those from Sample350-un increase till 450 °C and then remain stable. The percentages of $C_{6–14}$ from Sample350-un are overall higher than those from Sample350-ex and reach to a maximum at higher temperature at about 475 °C.

3.4 Pyrolysis products from the kerogen

Compositionally, properties of organic matters in Sample-k are similar to those in Sample0-ex. The only difference between the two samples is that inorganic minerals in Sample-k have been washed out. Evolution of hydrocarbon generation from Sample-k is shown in Fig. 4. Total yield reaches a maximum at about 525 °C, which is earlier than Sample0-ex, and decreases slightly at higher heating temperatures. Unlike whole-rock samples whose C_1 yields decrease at high temperatures, C_1 yield of kerogen keeps increasing and reaches 110.03 mg/g TOC at 600 °C. The maximum of $C_{2–5}$ fraction occurs around 500 °C, and that of $C_{6–14}$ fraction occurs at about 525 °C. Hydrocarbon yields at low temperatures are dominated by C_{15+} fraction. C_{15+} yield increases with increasing temperature and reaches a plateau at about 400 °C. It decreases significantly after temperature reaches

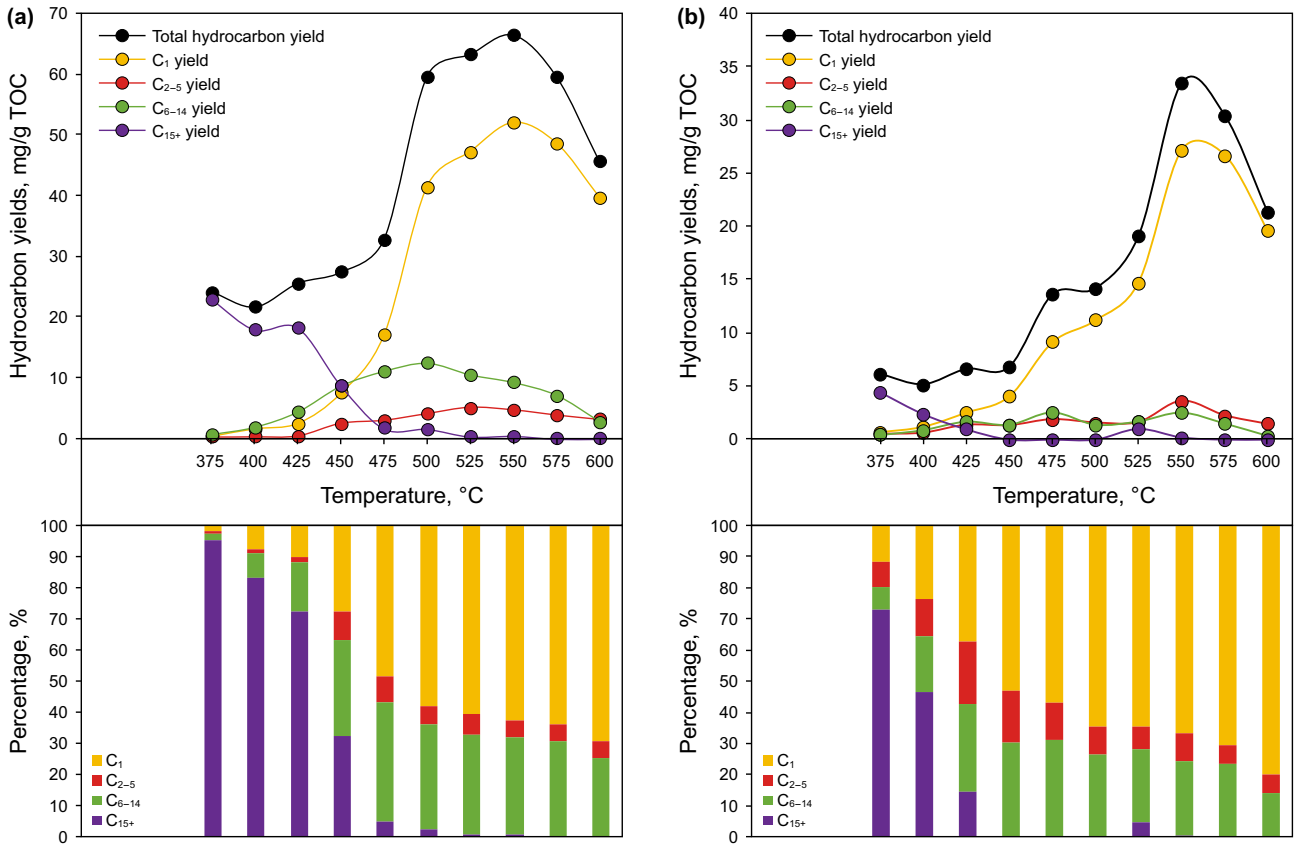

Fig. 3 Cumulative yields and percentages of C_1, $C_{2–5}$, $C_{6–14}$ and C_{15+} from MSSV pyrolysis of Sample350-un (**a**) and Sample350-ex (**b**)

450 °C. At high-temperature range (> 500 °C), light hydrocarbon fractions are dominant products.

According to the histogram showing the percentage of hydrocarbon yields from Sample-k, ratios of $C_{1–5}$, $C_{6–14}$ and C_{15+} remain unchanged when heating temperatures exceed 500 °C (Fig. 4). The percentages of $C_{1–5}$, $C_{6–14}$ and C_{15+} hydrocarbons at 600 °C are 76.75%, 16.79% and 6.45%, respectively. Also, compared to Sample0-ex, percentages of heavy C_{15+} components from Sample-k are obviously higher at low-temperature ranges. The differences between whole-rock samples and kerogen on yields of hydrocarbon products during heating indicate that inorganic rock fabrics could have been involved in hydrocarbon generation during closed-system pyrolysis.

4 Discussion

4.1 Hydrocarbon generation characteristics at different maturity

Depolymerization reaction of kerogen and heavy hydrocarbons, C–C bond cracking of C_{6+} saturated chains, demethylation reaction of aromatic structures and C–C bond cracking of $C_{3–5}$ aliphatic chains are four typical processes of thermal cracking of kerogens (Behar et al. 1992). The relative contributions from different hydrocarbon generation reactions through thermal maturation of shale remain a subject undergoing intense study (Tian et al. 2006; Vu et al. 2008; Guo et al. 2009).

MSSV yield of C_{15+} hydrocarbon from Sample325-un reduces slowly at low temperatures, followed by rapid decrease with high temperatures, indicating that a thermal maturity threshold is required for the cracking of heavy components. To find out the differences between hydrocarbons generated from retained oils with different thermal maturities, hydrocarbon yields from retained oil were calculated and are listed in Table 2 and Fig. 5. Compared with Sample350-un, retained oil in Sample325-un comprises higher contents of resin and asphaltene. C_{15+} yields from retained oil in Sample325-un and Sample350-un are similar. Yields of C_1, $C_{2–5}$ and $C_{6–14}$ generated from retained oil in samples heated to 325 °C are larger than those from samples heated to 350 °C. This is in agreement with previous studies reporting that resins and asphaltenes are main sources for saturates and aromatics (Ruble et al. 2001; Spigolon et al. 2015). The rapid increase of $C_{6–14}$ fractions generated from retained oil begins at 400 °C, while that of C_1 occurs at 450 °C.

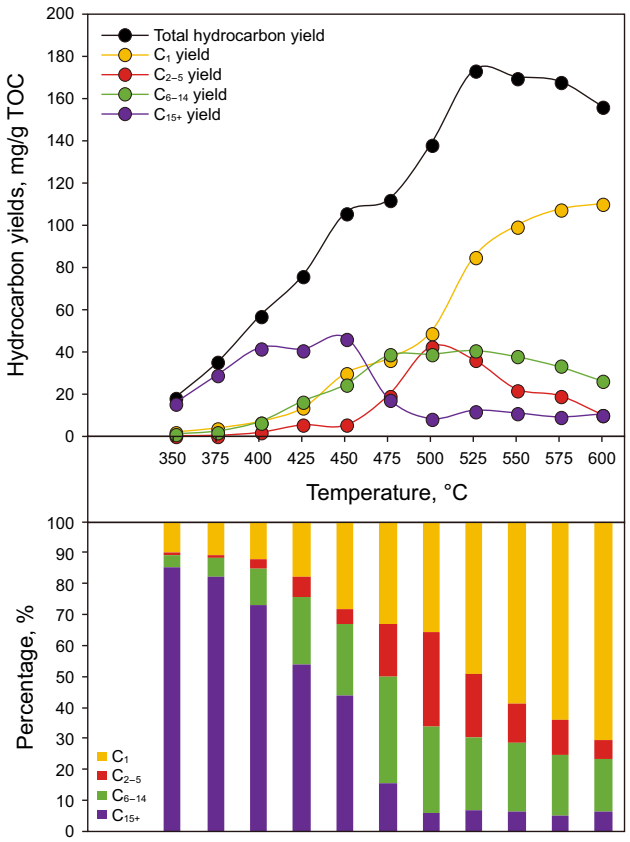

Fig. 4 Cumulative yields and percentages of C_1, C_{2-5}, C_{6-14} and C_{15+} from MSSV pyrolysis of Sample-k

Additionally, largest differences between C_{6-14}, C_{2-5}, C_1 yields from retained oils in Sample325-un and Sample350-un occur at 550 °C, 500 °C, 475 °C, respectively (dashed lines in Fig. 5). The above reflects that heavy hydrocarbons crack first into C_{6-14} and then gaseous light hydrocarbons during thermal maturation.

C_{15+} generation potentials of kerogens in Sample325 and Sample350 are almost depleted according to their measured Ro. Therefore, evolution trends of hydrocarbon yields from Sample325-un and Sample350-un can reflect the cracking of C_{15+} hydrocarbons that retained in shales. In general, the ends of rapid decreases of C_{15+} hydrocarbons correspond with the peaks of C_{6-14} yields in Sample325-un and Sample350-un, and the peaks of C_{2-5} yields typically occur at higher temperature than those of C_{6-14} hydrocarbons. Also, these C_{2-5} peaks in extracted samples appear at higher temperatures than in unextracted samples. Therefore, we could speculate a sequence of heavy hydrocarbon cracking in the studied Es_3 shale and that light hydrocarbons at high-maturity stage are from different origins.

Methane is the main gaseous product for all samples in this study, especially at high thermal maturities. Whether methane is predominately generated by oil cracking or kerogen cracking has always been a hot research topic, and a lot of studies in laboratory and analyses on field gas samples has been performed (Behar et al. 1992, 2008; Guo et al. 2009; Prinzhofer and Huc 1995; Wang et al. 2013). According to the yield results of unextracted samples in our study, increases of C_1 yields at high heating temperatures are accompanied by decreases of C_{2-5} yields. In contrast, this is not the same in extracted samples, where both C_1 and C_{2-5} yields increase or C_{2-5} yields remain generally stable (Figs. 1, 2, 3). As suggested by previous studies, the process of oil cracking includes (1) long-chain aliphatic hydrocarbons into mainly C_{2-5} wet gas with a small amount of C_1 at early stage and (2) C_{2-5} further cracking into C_1 in late stage (Behar et al. 1992; Hill et al. 2003). Therefore, C_1 in extracted samples is mainly generated from primary kerogen cracking, and contribution from the C–C bond cracking of C_{2-5} is limited. The rapid increases of C_1 yields from unextracted samples at high-maturity range are from both the cracking of kerogen and C_{2-5}, with the latter being the primary.

4.2 Influences of retained oil at early-mature stage on hydrocarbon generation at high-maturity stage

Original organic matters convert into different hydrocarbon fractions during thermal maturation, and kerogens and retained oil in shales act as intermediates in this process (Behar et al. 1992; Guo et al. 2009). Kerogens and oils formed at low-maturity stage can be regarded as sources of further hydrocarbon generation. Interaction between residual oil and kerogens at low-maturity stage is thought to have direct influences on potential and compositional properties of lately generated hydrocarbons (Erdmann and Horsfield 2006; McNeil and BeMent 1996; Dieckmann et al. 2006).

In this study, the ratios of light (C_{1-5}) to heavy (C_{6+}) hydrocarbons are applied to study the influences of retained oil in shales at low-maturity stage on hydrocarbon generation at high-maturity stage (Fig. 6). C_{1-5}/C_{6+} ratios of all samples increase slowly below 550 °C and relatively fast at higher temperatures. This is because heavy hydrocarbons are primary products at relative low temperature, and gas is the major product at high temperature. The C_{1-5}/C_{6+} ratios of Sample325-ex and Sample350-ex climb to rather high values rapidly after temperature reach above 550 °C, suggesting that these two samples are more prone to yield gas. The two samples have rather low C_{6+} yields during heating, and thus C_{1-5} yields can be roughly considered as derived from kerogens. In the classical hydrocarbon generation model proposed by Tissot and Welte (1978), all liquid hydrocarbons are destined to crack into gas at a given temperature. Therefore, it is reasonable to inferred that residual oil at

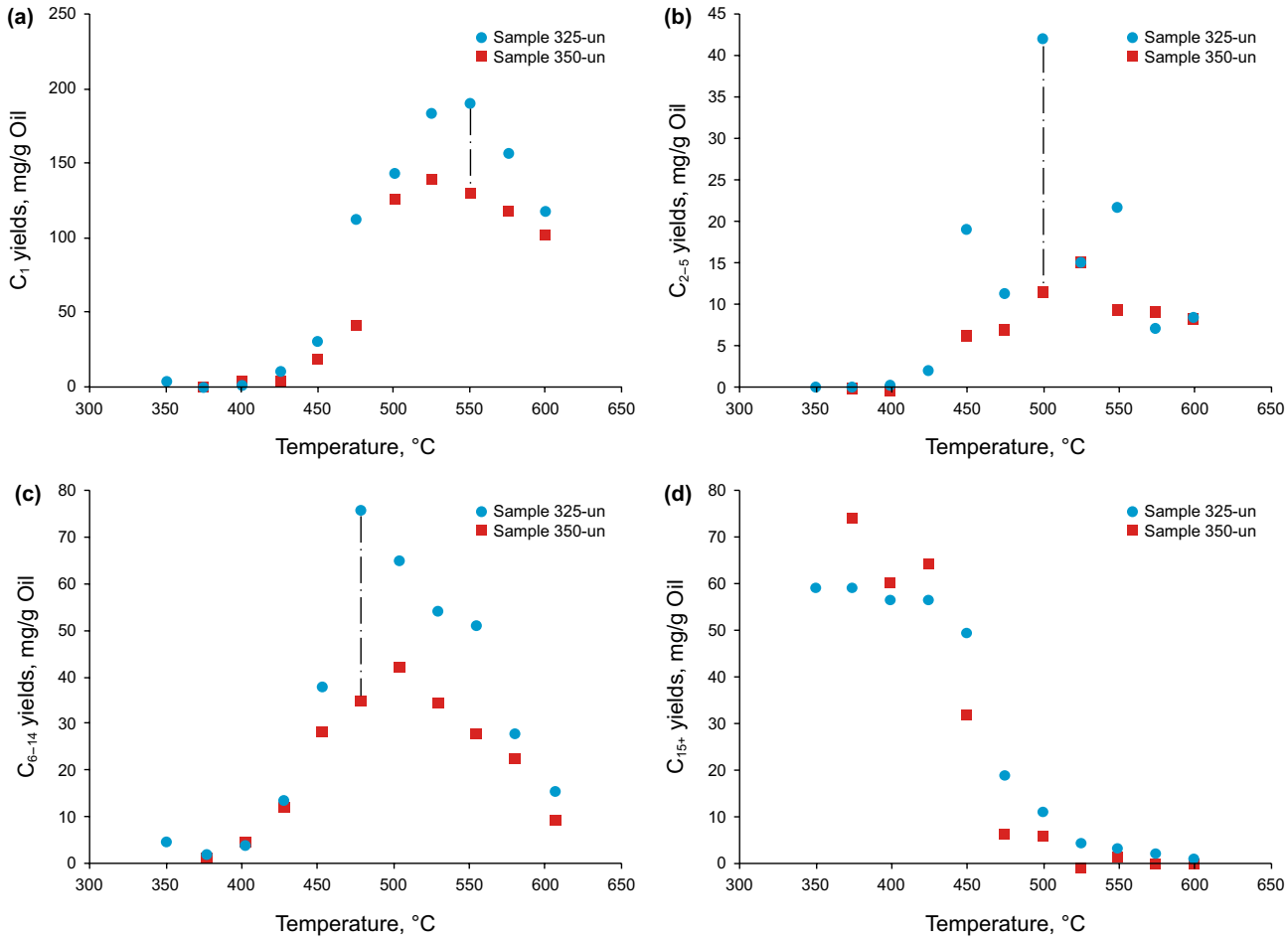

Fig. 5 Hydrocarbon yields from retained oils in Sample325-un and Sample350-un: **a** C_1 yield; **b** C_{2-5} yield; **c** C_{6-14} yield; **d** C_{15+} yield

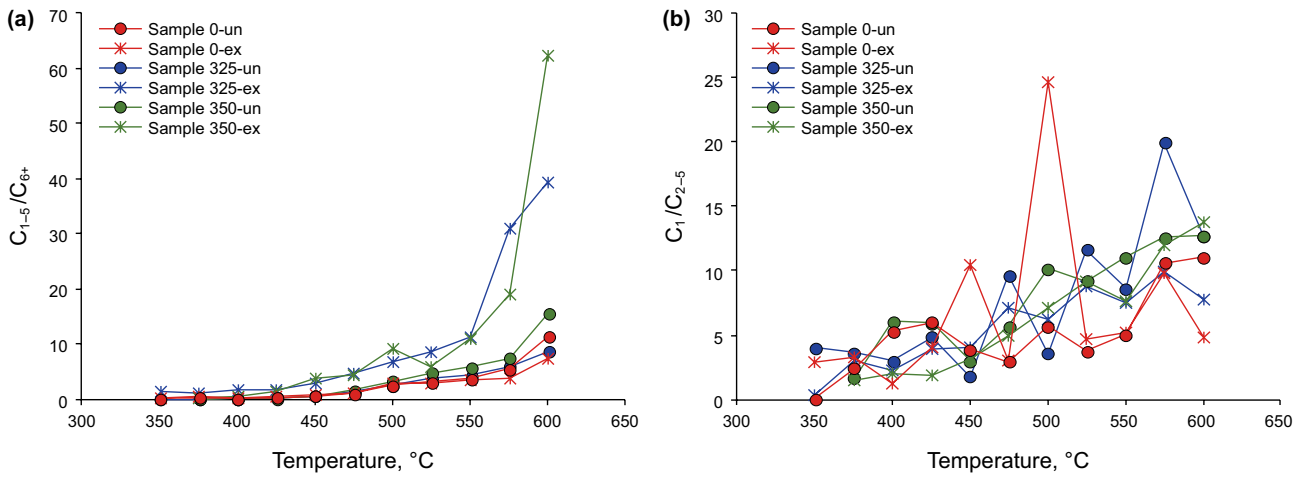

Fig. 6 Evolution of C_{1-5}/C_{6+} (**a**) and C_1/C_{2-5} (**b**) ratios in MSSV pyrolysis

early-mature stage may delay or extend the process of gas release at high-maturity stage in shales.

To figure out whether early retained oil in shales influences cracking of C_{2-5}, the changes of C_1/C_{2-5} during thermal maturation were studied. C_1/C_{2-5}-values of the

whole-rock samples increase from low to high heating temperatures with fluctuations (Fig. 6b), which can be attributable to the contributions from both the generation of C_{2-5} and transformation from C_{2-5} to C_1. Sample325-un, which contain the highest content of residual oil, has larger C_1/C_{2-5} values than Sample325-ex when heating temperatures exceed 525 °C. Gas products from Sample350-un are slightly dryer than those from Sample350-ex, when heating temperature exceeds 475 °C. This reflected that residual oil may prompt the cracking of C_{2-5} to C_1, while the effect is not quite distinct. As mentioned in previous studies, the absorption of retained oil into kerogen structures dominated by aromatic rings at low-maturity stage affects the release of methane at high-maturity stage (Gai et al. 2015; Pan et al. 2012; McNeil and BeMent 1996). The unheated sample in this study contains type I kerogens and minor type III kerogens and is thus dominated by aliphatic chains with minor aromatic groups. Kerogens in artificially matured Sample325 and Sample350 contain more aromatic clusters, due to higher thermal maturity. Therefore, changes of kerogen structures during thermal maturation affect the interaction between hydrocarbon products and kerogens and further influence late gas generation.

Hydrocarbon products generated during thermal maturation become progressively enriched in light component with heavy components disappearing gradually. In this process, the residual oil in shales may affect late hydrocarbon generation by buffering liquid hydrocarbons to gas and accelerating the cracking of C_{2-5} to methane moderately.

4.3 Loss of hydrocarbon yields during thermal maturation

A phenomenon worth noticing in our experimental work is that total and C_1 yields show significant decreases at high heating temperatures, which is different from previous work from other researchers (Horsfield and Dueppenbecker 1991; Behar et al. 1992; Li et al. 2018). There are two potential reasons for this: (1) transformation from volatile hydrocarbons to gas and coke; (2) reaction between inorganic materials in rocks and hydrocarbons.

It is widely accepted that hydrocarbons transform to dry gas and coke at postmature stage of thermal evolution of source rock (Tissot and Welte 1978; Horsfield et al. 1992). This is a possible explanation for the reducing yields of C_{2+} hydrocarbons. With regard to methane, which is relatively stable and decomposes only at extremely high temperature over 1000 °C without oxygen, more reasonable explanation needs to be given. Inasmuch as neither did we have temperature above 1000 °C, nor complete isolation from oxygen in the experiment.

As a self-generation and self-accumulation system, a variety of reactions between fluid and rock fabrics take place in shale reservoir during thermal maturation. Mineral composition as well as rock texture is involved in the processes of hydrocarbon generation and retention in shales, physically and chemically (Rahman et al. 2018; Shao et al. 2018a, b; Lewan et al. 2014). Thermochemical sulfate reduction (TSR) is a thermally driven reaction between hydrocarbons and sulfates and has been reported to be responsible for high H_2S concentrations in many petroleum accumulations (Krouse et al. 1988; Orr 1974; Worden et al. 1995; Cross et al. 2004). Theoretically, the reaction can occur at temperatures exceeding 25 °C (Amurskii et al. 1977; Worden and Smalley 1996; Schenk and Horsfield 1993). In geological conditions, the initiation of the reaction at much higher temperatures is reported, according to studies on petroleum reservoirs having experienced TSR (Krouse et al. 1988; Worden et al. 1995; Machel et al. 1995):

$$SO_4^{2-} + CH_4 \rightarrow CO_2 + H_2S + 2OH^- \text{ (methane as an example)} \quad (1)$$

The selected sample in this study contains 15wt% gypsum, which is unstable under high temperature and can be a potential source of sulfur. Therefore, it is plausible to consider that TSR was involved in the experiment and resulted in the decrease of cumulative hydrocarbon yields. To testify the speculation, a comparison is made between Sample-k and Sample0-ex. One of the salient differences between two samples is the evolution of methane yield at high temperature: methane yield from Sample-k increases till 600 °C and tends to be stable, while that from Sample0-ex shows a rapid decrease after reaching its maximum at 525 °C. By looking over the total yields from two samples, we can find that hydrocarbon yields from Sample-k are much larger than those from whole-rock samples. This is a strong evidence suggesting that hydrocarbon was consumed by mineral components in shales during thermal maturation. Figure 7 shows the percentage decreases of C_1 and total yields of the studied samples according to the ratio of final yield to maximum yield. It is interesting that the decreases of C_1 and total yields from Sample350 series are smaller than those from Sample0-ex and Sample325 series. This could be attributed to loss of gypsum during sample preparation by heating samples in semi-open hydrous pyrolysis system. In addition, percentage decreases of hydrocarbon yield in extracted samples are higher than those in unextracted samples, and loss of hydrocarbon yields in Sample0-un is minimal (Fig. 7). Hence, it can be inferred that TSR occurred during our experiments (there may not be enough gypsum for the consumption of larger amount of hydrocarbon products from unextracted samples). Whether this TSR reaction occurs in shale oil/gas layers under geological conditions remains to be examined and further works on natural shale samples are necessary. If TSR has an influence on hydrocarbon generation in shale layers when the burial depth is

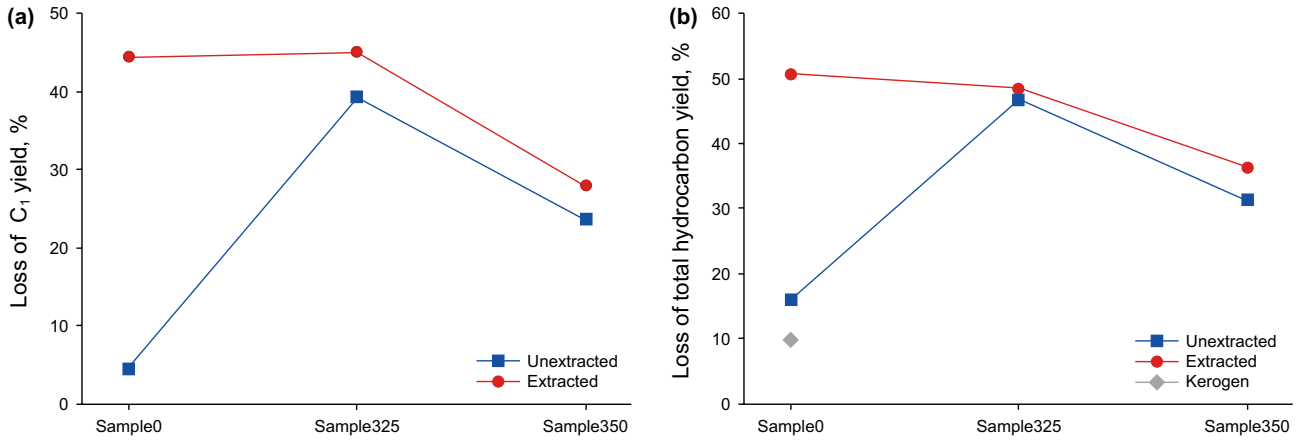

Fig. 7 Percentage decreases at high heating temperatures of C_1 (**a**) and total hydrocarbon (**b**) yields of the studied samples

large enough, a practical implication from the above is that great caution should be taken when evaluating hydrocarbon resources from deep-buried gypsum-bearing shale system.

5 Conclusions

By conducting MSSV pyrolysis experiments on artificially matured lacustrine shale samples, we studied hydrocarbon generation characteristics of shales with the influence of retained oil. Hydrocarbon yields from samples with or without retained oil at different thermal maturities follow different evolution paths. Total yields of all whole-rock samples reach their maximum at heating temperature of about 550 °C, followed by significant decreases. Maximal total yield of kerogen sample occurs around 525 °C and decreases slightly afterward. Besides, evolutions of C_{2-5}, C_{6-14} and C_{15+} yields vary from sample to sample. The cracking of C_{15+} in the studied lacustrine shales generally follows a sequence as they first transform into C_{6-14} liquid hydrocarbons and then further crack into C_{2-5} gaseous hydrocarbons. Methane is the major gas product in all samples, and there are different origins. Cracking of C_{2+} is the major origin for methane generation in shales with retained oil, while methane in extracted shale samples is largely contributed from primary kerogen cracking. In the studied lacustrine shale samples, the process of oil transforming to gas is extended by oil retained at low-maturity stage. In addition, retained oil may also slightly prompt the cracking of C_{2-5} to methane. Gypsum in samples is responsible for most of the hydrocarbon loss during heating, especially at high temperatures. Conversion of volatile hydrocarbons to gas and coke can be a secondary factor resulting in the decrease of C_{2+} yield at high heating temperatures.

Acknowledgements This research was funded by National Natural Science Foundation of China (No. 41872148) and China Major Research and Development Program for Oil and Gas (No. 2017ZX05049001). Xinhe Shao acknowledges the financial supporting from China Scholarship Council and American Association of Petroleum Geologists (Norman H. Foster Memorial Grant). We thank Sinopec Zhongyuan Oilfield Company for providing samples and background geological data in this study.

References

Amurskii GI, Goncharov ES, Zhabrev IP, et al. Genesis of H_2S-containing natural gases of oil and gas basins. Soviet Geol. 1977;5:56–68.

Behar F, Kressmann S, Rudkiewicz JL, et al. Experimental simulation in a confined system and kinetic modelling of kerogen and oil cracking. Org Geochem. 1992;19(1–3):173–89. https://doi.org/10.1016/0146-6380(92)90035-V.

Behar F, Lorant F, Lewan M. Role of NSO compounds during primary cracking of a Type II kerogen and a Type III lignite. Org Geochem. 2008;39(1):1–22. https://doi.org/10.1016/j.orggeochem.2007.10.007.

Braun RL, Burnham AK, Reynolds JG, et al. Pyrolysis kinetics for lacustrine and marine source rocks by programmed micropyrolysis. Energy Fuels. 1991;5(1):192–204. https://doi.org/10.1021/ef00025a033.

Burnham AK. A simple kinetic model of petroleum formation and cracking (No. UCID-21665). Lawrence Livermore National Lab., CA (USA). 1989.

Cross MM, Manning DA, Bottrell SH, et al. Thermochemical sulphate reduction (TSR): experimental determination of reaction kinetics and implications of the observed reaction rates for petroleum reservoirs. Org Geochem. 2004;35(4):393–404. https://doi.org/10.1016/j.orggeochem.2004.01.005.

Dieckmann V, Ondrak R, Cramer B, et al. Deep basin gas: new insights from kinetic modelling and isotopic fractionation in deep-formed gas precursors. Mar Pet Geol. 2006;23(2):183–99. https://doi.org/10.1016/j.marpetgeo.2005.08.002.

Erdmann M, Horsfield B. Enhanced late gas generation potential of petroleum source rocks via recombination reactions: evidence from the Norwegian North Sea. Geochim Cosmochim Acta. 2006;70(15):3943–56. https://doi.org/10.1016/j.gca.2006.04.003.

Gai H, Xiao X, Cheng P, et al. Gas generation of shale organic matter with different contents of residual oil based on a pyrolysis experiment. Org Geochem. 2015;78:69–78. https://doi.org/10.1016/j.orggeochem.2014.11.001.

Guo L, Xiao X, Tian H, et al. Distinguishing gases derived from oil cracking and kerogen maturation: insights from laboratory pyrolysis experiments. Org Geochem. 2009;40(10):1074–84. https://doi.org/10.1016/j.orggeochem.2009.07.007.

Han Y, Mahlstedt N, Horsfield B. The Barnett Shale: compositional fractionation associated with intraformational petroleum migration, retention, and expulsion. AAPG Bull. 2015;99(12):2173–202. https://doi.org/10.1306/06231514113.

Hill RJ, Tang Y, Kaplan IR. Insights into oil cracking based on laboratory experiments. Org Geochem. 2003;34(12):1651–72. https://doi.org/10.1016/S0146-6380(03)00173-6.

Horsfield B, Dueppenbecker SJ. The decomposition of Posidonia Shale and Green River Shale kerogens using microscale sealed vessel (MSSV) pyrolysis. J Anal Appl Pyrol. 1991;20:107–23. https://doi.org/10.1016/0165-2370(91)80066-H.

Horsfield B, Disko U, Leistner F. The micro-scale simulation of maturation: outline of a new technique and its potential applications. Geol Rundsch. 1989;78(1):361–73.

Horsfield B, Schenk HJ, Mills N, et al. An investigation of the in-reservoir conversion of oil to gas: compositional and kinetic findings from closed-system programmed-temperature pyrolysis. Org Geochem. 1992;19(1–3):191–204. https://doi.org/10.1016/0146-6380(92)90036-W.

Jarvie DM, Hill RJ, Ruble TE, et al. Unconventional shale-gas systems: the Mississippian Barnett Shale of north-central Texas as one model for thermogenic shale-gas assessment. AAPG Bull. 2007;91(4):475–99. https://doi.org/10.1306/12190606068.

Jia W, Wang Q, Liu J, et al. The effect of oil expulsion or retention on further thermal degradation of kerogen at the high maturity stage: a pyrolysis study of type II kerogen from Pingliang shale, China. Org Geochem. 2014;71:17–29. https://doi.org/10.1016/j.orggeochem.2014.03.009.

Krouse HR, Viau CA, Eliuk LS, et al. Chemical and isotopic evidence of thermochemical sulphate reduction by light hydrocarbon gases in deep carbonate reservoirs. Nature. 1988;333(6172):415–9.

Lewan MD, Roy S. Role of water in hydrocarbon generation from Type-I kerogen in Mahogany oil shale of the Green River Formation. Org Geochem. 2011;42(1):31–41. https://doi.org/10.1016/j.orggeochem.2010.10.004.

Lewan MD, Dolan MP, Curtis JB. Effects of smectite on the oil-expulsion efficiency of the Kreyenhagen Shale, San Joaquin Basin, California, based on hydrous-pyrolysis experiments. AAPG Bull. 2014;98(6):1091–109. https://doi.org/10.1306/10091313059.

Li J, Wang W, Cao Q, et al. Impact of hydrocarbon expulsion efficiency of continental shale upon shale oil accumulations in eastern China. Mar Pet Geol. 2015;59:467–79. https://doi.org/10.1016/j.marpetgeo.2014.10.002.

Li X, Krooss BM, Ostertag-Henning C, et al. Liberation of hydrogen-containing gases during closed system pyrolysis of immature organic matter-rich shales. Int J Coal Geol. 2018;85:23–32. https://doi.org/10.1016/j.coal.2017.11.001.

Machel HG, Krouse HR, Sassen R. Products and distinguishing criteria of bacterial and thermochemical sulfate reduction. Appl Geochem. 1995;10(4):373–89. https://doi.org/10.1016/0883-2927(95)00008-8.

Mahlstedt N, Horsfield B, Dieckmann V. Second order reactions as a prelude to gas generation at high maturity. Org Geochem. 2008;39(8):1125–9. https://doi.org/10.1016/j.orggeochem.2008.04.011.

McNeil RI, BeMent WO. Thermal stability of hydrocarbons: laboratory criteria and field examples. Energy Fuels. 1996;10(1):60–7. https://doi.org/10.1021/ef9501399.

Orr WL. Changes in sulfur content and isotopic ratios of sulfur during petroleum maturation—study of Big Horn Basin Paleozoic oils. AAPG Bull. 1974;58(11):2295–318. https://doi.org/10.1306/83D91B9B-16C7-11D7-8645000102C1865D.

Pan C, Jiang L, Liu J, et al. The effects of pyrobitumen on oil cracking in confined pyrolysis experiments. Org Geochem. 2012;45:29–47. https://doi.org/10.1016/j.orggeochem.2012.01.008.

Peters KE, Walters CC, Mankiewicz PJ. Evaluation of kinetic uncertainty in numerical models of petroleum generation. AAPG Bull. 2006;90(3):387–403. https://doi.org/10.1306/10140505122.

Prinzhofer AA, Huc AY. Genetic and post-genetic molecular and isotopic fractionations in natural gases. Chem Geol. 1995;126(3–4):281–90. https://doi.org/10.1016/0009-2541(95)00123-9.

Rahman HM, Kennedy M, Löhr S, et al. The influence of shale depositional fabric on the kinetics of hydrocarbon generation through control of mineral surface contact area on clay catalysis. Geochim Cosmochim Acta. 2018;220:429–48. https://doi.org/10.1016/j.gca.2017.10.012.

Ruble TE, Lewan MD, Philp RP. New insights on the Green River petroleum system in the Uinta basin from hydrous pyrolysis experiments. AAPG Bull. 2001;85(8):1333–71. https://doi.org/10.1306/8626CAB9-173B-11D7-8645000102C1865D.

Schenk HJ, Horsfield B. Kinetics of petroleum generation by programmed-temperature closed-versus open-system pyrolysis. Geochim Cosmochim Acta. 1993;57(3):623–30. https://doi.org/10.1016/0016-7037(93)90373-5.

Shao D, Ellis GS, Li Y, et al. Experimental investigation of the role of rock fabric in gas generation and expulsion during thermal maturation: anhydrous closed-system pyrolysis of a bitumen-rich Eagle Ford Shale. Org Geochem. 2018a;119:22–35. https://doi.org/10.1016/j.orggeochem.2018.01.012.

Shao X, Pang X, Li H, et al. Pore network characteristics of lacustrine shales in the Dongpu Depression, Bohai Bay Basin, China, with implications for oil retention. Mar Pet Geol. 2018b;96:457–73. https://doi.org/10.1016/j.marpetgeo.2018.06.015.

Shao X, Pang X, Li M, et al. Hydrocarbon retention in lacustrine shales during thermal maturation: insights from semi-open system pyrolysis. J Pet Sci Eng. 2020;184:106480. https://doi.org/10.1016/j.petrol.2019.106480.

Sondergeld CH, Rai CS, Curtis ME. Relationship between organic shale microstructure and hydrocarbon generation. In: SPE unconventional resources conference-USA. Society of Petroleum Engineers. 2013, April. https://doi.org/10.2118/164540-MS.

Spigolon AL, Lewan MD, de Barros Penteado HL, et al. Evaluation of the petroleum composition and quality with increasing thermal maturity as simulated by hydrous pyrolysis: a case study using a Brazilian source rock with Type I kerogen. Org Geochem. 2015;83:27–53. https://doi.org/10.1016/j.orggeochem.2015.03.001.

Tian H, Wang Z, Xiao Z, et al. Oil cracking to gases: kinetic modeling and geological significance. Chin Sci Bull. 2006;51(22):2763–70. https://doi.org/10.1007/s11434-006-2188-8.

Tissot BP, Welte DH. Petroleum formation and occurrence: a new approach to oil and gas exploration. Berlin: Springer; 1978. p. 538.

Vu TA, Horsfield B, Sykes R. Influence of in situ bitumen on the generation of gas and oil in New Zealand coals. Org Geochem. 2008;39(11):1606–19. https://doi.org/10.1016/j.orggeochem.2008.07.005.

Wang Q, Lu H, Greenwood P, et al. Gas evolution during kerogen pyrolysis of Estonian Kukersite shale in confined gold tube system. Org Geochem. 2013;65:74–82. https://doi.org/10.1016/j.orggeochem.2013.10.006.

Worden H, Smalley PC. H_2S-producing reactions in deep carbonate gas reservoirs: Khuff Formation, Abu Dhabi. Chem Geol. 1996;133(1–4):157–71. https://doi.org/10.1016/S0009-2541(96)00074-5.

Worden H, Smalley C, Oxtoby NH. Gas souring by thermochemical sulfate reduction at 140. AAPG Bull. 1995;79(6):854–63.

Wu Y, Ji L, He C, et al. The effects of pressure and hydrocarbon expulsion on hydrocarbon generation during hydrous pyrolysis of type-I kerogen in source rock. J Nat Gas Sci Eng. 2016;34:1215–24. https://doi.org/10.1016/j.jngse.2016.08.017.

Ziegs V, Horsfield B, Skeie JE, et al. Petroleum retention in the mandal formation, central Graben, Norway. Mar Pet Geol. 2017;83:195–214. https://doi.org/10.1016/j.marpetgeo.2017.03.005.